J. Indian Chem. Soc.,
Vol. 81, August 2004, pp. 644-653

Kinetics of thermal dehydration and decomposition of hydrated chlorides of some 3d transition metals (Mn-Cu series). Part-I. Dehydration of $MnCl_2.4H_2O$

S. B. Kanungo*

Regional Research Laboratory, Bhubaneswar-751 013, India

Manuscript received 4 July 2003, revised 9 March 2004, accepted 10 March 2004

The thermal dehydration of $MnCl_2$ hydrate has been studied by using simultaneous TG/DTA under the static air (or self-generated atmosphere) and also under the flowing nitrogen condition at different heating rates. In either of the above condition the salt dehydrates in three steps, with the losses of about 1.0, 1.2 and 1.1 moles of water in static air and 0.9, 2.1 and 1.1 moles of water in flowing nitrogen atmosphere. The heats of the three steps of dehydration in air have been estimate2d from area under the corresponding DTA peaks at the heating rate of 10°/min. The first step of dehydration is accompanied with the melting of the salt and therefore does not follow any kinetic model of solid state decomposition. For the other two steps of dehydration changes in the mechanism are observed and attempts have been made to identify these changes. All these have been possible by converting non-isothermal time into isothermal time which is more appropriate in the kinetic analysis. It is observed that either nucleation and growth or progress of the reactant/product interface is generally the most suitable kinetic model for the dehydration of manganese chloride hydrate.

Hydrated crystalline salts form one of the earliest class of compounds used as models for the study of thermally stimulated solid-state reactions. The ease with which water is removed from the coordination sphere of metal ion at relatively low temperature and the distinct crystalline features of both hydratd and dehydrated salts have led to extensive investigation of this class of compounds. A few review articles have appeared on this subject[1–3].

Water acts as a strong coordinating ligand with many positive ions not only in their aqueous solutions, but also in the crystalline structures of the salts of their cations. It may, however, be emphasized that the water which constitutes aquo ion (usually hexaaquo) may not be present in the crystalline hydrates as the limitations imposed by the crystal structure allow some H_2O molecules to be strongly bonded than others. Some crystalline hydrates may undergo melting, eutectic transformation or dissolution in one of the products. In such cases, the rate of dehydration is altered due to relaxation of intermolecular binding forces that exist in the crystalline solid[1]. As a result, melting brings about supercooling effect on the dehydration process which renders the determination of true kinetic parameters difficult.

The hydrated chlorides of transition metals (Mn-Cu series) exhibit considerable variation not only in the number of water molecules per molecule of salt, but also in their thermal dehydration behavior. Most of the salts dehydrate in three stages with the loss of varying number of moles of water in each stage depending upon the water molecules per molecule of salt present in the initial stage[4–7]. Generally, the first stage of the loss of water is accompanied by melting of the salt and the subsequent dehydration takes place from the product phase which is either a tetrahydrate or a dihydrate. But $CuCl_2.2H_2O$ dehydrates in one step[6–8]. Further, while the anhydrous chlorides of Mn and Fe^{II} tend to volatilize at higher temperature before decomposition, anhydrous salts of Co, Ni and Cu decompose to their oxides by dehydrochlorination and/or dechlorination. Our interest in thermal dehydration and decomposition of the hydrated chlorides of the transition metals originates from the chloridising roasting of Ni and Co bearing lateritic ores and Ni, Co, Cu and Zn containing manganese nodules. Though iron does not occur in these minerals as Fe^{II}, dehydration of $FeCl_2.4H_2O$ has also been studied for the sake of completion of the work on this series of hydrated chlorides. In this regard, we have studied thermal dehydration and decomposition characteristics of the hydrated chlorides of Ni[9,10], Co[11] and Fe^{III} [12,13]. In the present series of work an attempt has been made to study the kinetics of dehydration and decomposition of the hydrated chlorides of Mn, Fe^{II}, Co, Ni and Cu with a view to examine these data with decreasing ionic radii.

*Present address : Flat No. A7/2, Konnagar Abasan, Konnagar-712 235, Hooghly, West Bengal, India.

The present paper deals with dehydration kinetics of $MnCl_2.4H_2O$.

Results and discussion

Fig. 1 shows the TG and DTA traces of $MnCl_2.4H_2O$ at two typical heating rates (6° and 10°/min) under static air or self-generating atmosphere. It may be noted that the salt undergoes melting at temperature around 60° followed by the loss of about 1 mole of water at temperature around 70°. The sharpness of the first endothermic peak clearly suggests melting of the salt in its own water of hydration. The mass loss data corresponding to different moles of H_2O are given in Table 1.

The second step of dehydration involves a major loss of water with endothermic peak at temperature varying between 115 and 120°. This is followed by the third step of dehydration involving generally loss of about 1 mole of H_2O and characterized by DTA peak temperature varying between 164° and 183° depending upon the heating rate. It may be noted here that the total loss of H_2O in the three steps varies from 3.12 to 3.57 moles which is less than the actual H_2O present indicating that in air or self-generating atmosphere some water is retained by the final product. The relevant data are summarized in Table 1.

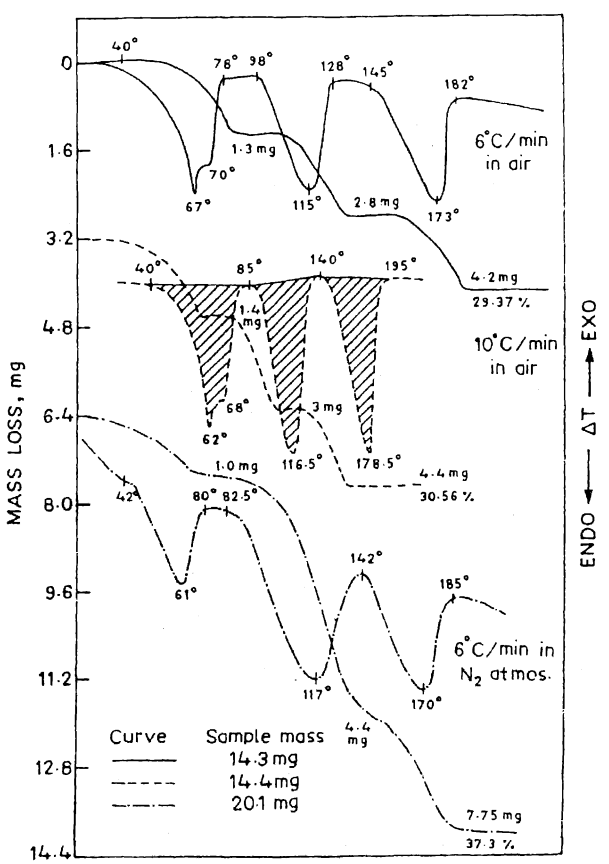

Fig. 1. Simultaneous TG/DTA traces of $MnCl_2.4H_2O$ in air and in flowing nitrogen atmosphere at one or two typical heating rates. The hatched areas under the DTA peaks at 10°/min in air are used for estimating heats of dehydration.

Fig. 1 also illustrates typical TG and DTA traces at 6°/min under flowing N_2 atmosphere. It can be seen that there is practically little or no change in the DTA peak temperature for the first step of dehydration. Table 1 shows that the number of moles of water lost in this step are lower than that obtained in static air. The peak temperatures of the second and the third steps of dehydration are lower than those observed under static air condition indicating that flowing N_2 facilitates removal of water vapor from the surface. The number of moles of water lost in the second step are much higher than in the static air while for the third step the values are almost similar. Thus, the total number of moles of water lost for the three steps together is about four. This shows that the dehydration of $MnCl_2$ hydrate under the static air is not complete. However, the dehydrated salt does not deompose and is vaporized at temperature above 800°.

Estimation of the heat of dehydration of $MnCl_2$ hydrate in air :

The heats of the three steps of dehydration of $MnCl_2.4H_2O$ in air have been estimated from the temperature and the area under the DTA peaks obtained by heating the salt at 10°/min. According to the principle of DTA, heat evolved or absorbed (ΔH/g) during any thermally stimulated process is proportional to area per unit weight under DTA peak[14] i.e.

$$\Delta H = k \times A/m \qquad (1)$$

where, A = area under the DTA peak, cm^2, m = mass of the sample, g and k = calibration constant, kJ/cm^2. Fig. 2 illustrates the calibration curve prepared by the thermolysis of various standard compounds whose heats of thermal transformation/decomposition are available in the literature[14]. The corresponding k values were calculated from eq. (1) and plotted against peak temperature. There are some obvious problems in this method. These arise from uncertainty in delineating exact peak area, difference in heat capacity between reactants and products, measurement error in sample temperature etc. which may together lead to an error of sometimes more than 15%. However, if the experiments are performed under carefully controlled conditions the overall error can be reduced to 10%. The heats of reaction for the different

Table 1. Effect of heating rate on the thermal dehydration parameters of $MnCl_2.4H_2O$

Heating rate C/min	First stage of dehydration			Second stage of dehydration			Third stage of dehydration			Total loss of H_2O moles
	Temp. range (Ti-Tc)# ℃	DTA peak temp. ℃	Moles of H_2O lost	Temp. range (Ti-Tc)# ℃	DTA peak temp. ℃	Moles of H_2O lost	Temp. range (Ti-Tc)# ℃	DTA peak temp. ℃	Moles of H_2O lost	
In static air environment :										
2	42.5–68.0	60.5	1.31	92.5–116	110	1.13	155–173	164	1.13	3.57
4	43–74	60.5, 65*	1.06	92–120	113	1.14	142–177	167.5	1.14	3.34
5	40–72	61, 66*	1.01	92.5–121	115	1.22	141.5–177.5	172	1.08	3.31
6	40–78	67, 70*	1.0	94–128	115	1.04	145–182	173	1.08	3.60
8	38–92	61, 70*	1.06	96–139	120	1.38	155–200	183	1.06	3.50
10	41–85	61, 68*	1.0	95–140	117	1.28	140–195	178.5	1.08	3.36
Nitrogen flow environment :										
2	45–65.5	60	0.93	87–121	1.2.5	2.2	135–166.5	163	1.10	4.3
4	38–70	60	0.95	85–135	108	2.2	138–180	163.5	1.13	4.26
6	40–70	61	1.00	82.5–142	117	1.89	142–185	170	1.13	4.02
8	38–75	60	0.62	84–145	115	2.13	145–200	174	1.18	3.93

*Weak but distinct endothermic peak.

#T_i = Temperature of inception of DTA peak T_e = Temperature of completion of DTA peak.

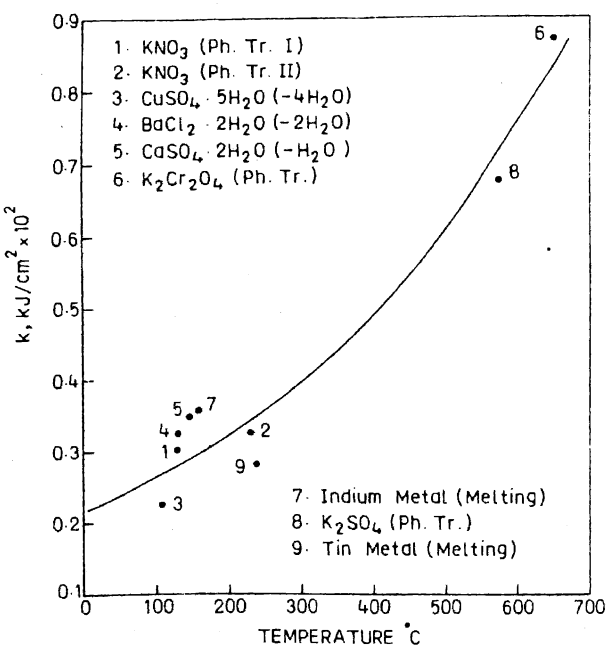

Fig. 2. Calibration curve of the instrument at 10°/min in air using several standand substances whose heats of transformation are known.

steps of dehydration are then estimated from the following relationship

$$\Delta H_{reac} = k\ (kJ/cm^2) \times A\ (cm^2/g) \times \text{molar mass of the product}$$

where, k = constant at the DTA peak temperature and is obtained from the calibration curve. The shaded areas under the three DTA peaks at 10°/min in Fig. 1 are used in the calculation of the heats absorbed for the three steps of dehydration of $MnCl_2.4H_2O$ in static air and the values are found to be 68.4, 89.8 and 81.6 kJ/mol of product respectively.

Kinetics of dehydration :

The study of the kinetics of dehydration of hydrated salts is beset with problem, especially for those where melting is evident. This aspect of thermal analysis has been critically examined by Galwey[3]. Initially an attempt was made to study the kinetics of dehydration reaction by the isothermal methods. But it was not successful because by the time temperature was stabilized a significant fraction of reaction had already taken place. Therefore, non-isothermal method has been used which provides reasonably precise data for the onset and completion of the different steps of dehydration which, however, are not possible to obtain by the isothermal method for this type of fast reaction. Even a very minute or subtle change in mechanism can be identified by non-isothermal method by varying experimental conditions such as heating rate, sample size, gaseous environment etc. A large number of methods have been developed during the last three decades on the study of the kinetics of solid state reactions under non-isothermal condition[1,15,16]. Many of these methods suffer from certain limitations and have been

subjected to criticism. It is now generally accepted that isoconversion method developed independently by Ozawa[17] in Japan and Flynn and Wall[18] in USA is free from many ambiguities and therefore has been used in the present work. The theoretical background of the OFW method is briefly discussed below as it is not yet widely used so far.

Theoretical background of the OFW method :

The basic equation for the kinetic analysis of a thermally stimulated process under linear heating rate can be expressed in the following well-known form

$$\int_0^{\infty} d\alpha/f(a) = g(\alpha) = A/b \int_{To}^{T} \exp(-E/RT)\, dT = AE/bR\, p(x) \qquad (2)$$

where, $g(\alpha)$ is the integrated form of the function $1/f(\alpha)$ which represents the mechanistic model equation for the reaction, A and E are the pre-exponential factor and activation energy as envisaged in the well-known Arrhenius equation, R is the molar gas constant, b is the linear heating rate (dT/dt) and $p(x)$ is the negative integral of the temperature function and is given by :

$$p(x) = \int e^{-x}/x^2\, d(x) \qquad (3)$$

where, $x = E/RT$. Taking logarithm on both sides of eq. (2) we have

$$\log g(x) - \log p(x) = \log (AE/bR) \qquad (4)$$

In the absence of any exact solution for $p(x)$ we may use the following Doyle's approximation (for $20 < x < 60$) as follows[19] :

$$\log p(x) = -2.315 - 0.4567x \qquad (5)$$

Substituting in eq. (2) and rearranging

$$\log b = \log [AE/Rg(\alpha)] - 2.315 - 0.4567\ (E/RT) \qquad (6)$$

If the mechanism of the thermal process does not change with variation in heating rate for a reasonably wide range of fractional conversion (α), a plot of $\log b$ vs $1/T$ should yield a series of straight lines for different values of α taken at suitable intervals. From these lines E values can be obtained which are independent of any mechanistic model. Ozawa[17] also introduced the term reduced time (θ) which is given by

$$\theta = (E/bR).p(x) \qquad (7)$$

Taking logarithm on both sides

$$\log \theta = \log (E/bR) + \log p(x) \qquad (8)$$

Substituting eq. (5) for the value of $\log p(x)$

$$\log \theta = \log (E/bR) - 2.315 - 0.4567\ (E/RT) \qquad (9)$$

By utilizing the mean E value obtained from the isoconversion curves at different α values, $\log \theta$ values can be calculated for a given heating rate. Similarly, from the $\log \theta$ values for at least three heating rates, a mean $\log \theta$ (or θ) for each values of α can be obtained.

Transformation of non-isothermal to isothermal decomposition :

By defination, for an isothermal process the reduced time θ can also be written as follows[20]

$$\theta = \int \exp(-E/RT)\, dt \qquad (10)$$

Differentiating and combining with Arrhenius equation

$$d\theta/dt = k/A = \text{constant} \qquad (11)$$

$$\text{or, } \theta = (k/A)\, t \qquad (12)$$

where k = specific rate-constant. Since, for an isothermal process T is constant we may reinvoke Arrhenius equation to obtain the following transformation.

$$\theta = \exp(-E/RT_{iso})\, t \qquad (13)$$

Taking logarithm and rearranging

$$\log t = \log \theta + (E/2.303\ RT_{iso}) \qquad (14)$$

In the light of the above theoretical background kinetics of the dehydration of $MnCl_2.4H_2O$ (and also other hydrated chlorides in the subsequent papers) have been discussed below. In all these studies each step of dehydration in TG curve is first carefully delineated and then converted to a (fractional conversion) vs temperature (K) curvs where α is defined as

$$\alpha = W - W_o/W_f - W_o$$

where, W_o, W and W_f are the mass losses (mg) in the beginning of the step, at any temperature within the step and at the end of the step, respectively.

The first step of dehydration of $MnCl_2$ hydrate in static air is accompanied with melting of the salt at about 61°. The subsequent dehydration possibly takes place from the moist surface or semi-solid phase. No meaningful kinetic parameter can be obtained from this step because of the variation in temperature that likely to occur during melting. The second step of dehydration in air shows loss of little more than one mole of water and the α vs temperature curves at different heating rates is illustrated in

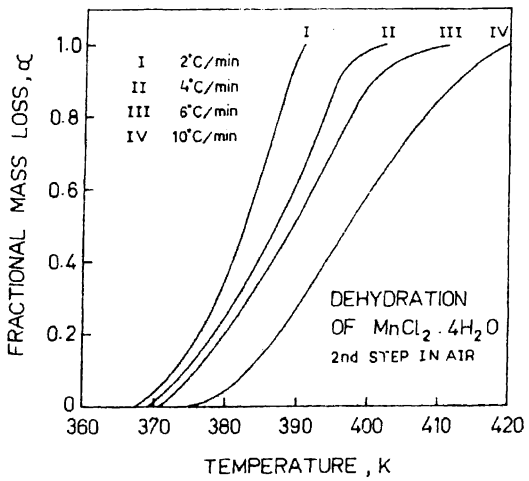

Fig. 3. Plot of α vs T for the second step of dehydration of tetrahydrate in air at different heating rates.

Fig. 3. The corresponding isoconversion plots in Fig. 4 show good linear behavior for 2°, 4° and 6°/min. There-

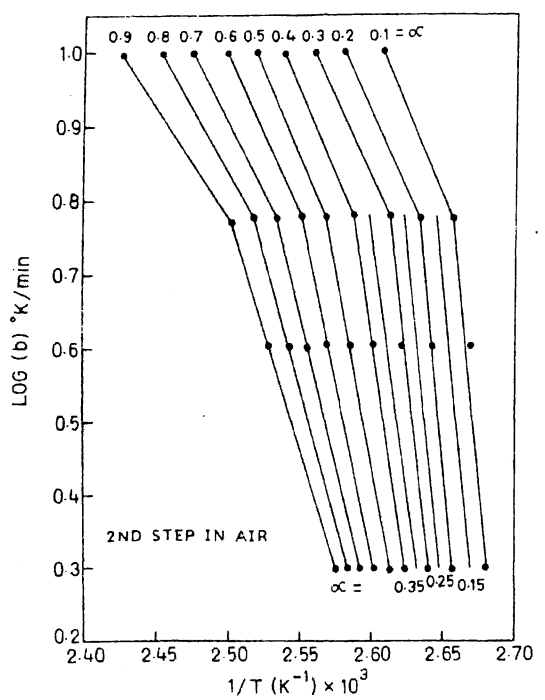

Fig. 4. Plot of log (heating rate) vs $1/T$ at different leaves of α i.e. isoconversion plot for the second step of dehydration in air.

fore, E values have been calculated from the first three heating rates using eq. (6). The results in Table 2 show wide variation from 345.8 kJ/mol at α = 0.1 to 118.3 kJ/mol at α = 0.9. Such high E values suggest strong binding of these water molecules either within themselves or with the central metal ion. It may also be noted that mecha-

Table 2. Activation energy values obtained by the isoconversion method for different steps of the dehydration of $MnCl_2.4H_2O$ in air and in flowing N_2 environment

	Dehydration in static air				Dehydration in flowing N_2 environment	
	2nd step		3rd step		2nd step	3rd step
	E values	Mean E	E values	Mean E	E values	E values
(α)	kJ/mol	kJ/mol	kJ/mol	kJ/mol	kJ/mol	kJ/mol
0.10	345.8		172.9[b]		80.9[d]	145.7[a]
0.15	336.7					
0.20	345.8		136.5[b]		83.0[d]	145.7[a]
0.25	309.4					
0.30	309.4		123.8[b]		69.9[d]	116.5
0.35	255.0	317.0				
0.40	218.0[a]		112.8[b]		65.5[d]	84.5
0.50	163.8		109.2[b]		85.2[e]	80.1
0.60	163.8		105.5[b]	126.8	83.7[e]	93.2
0.70	141.1		136.5[c]		76.5[e]	54.6
0.80	127.4		112.8[c]		75.6[e]	76.5
0.90	118.3	142.8	109.2[c]		67.0[e]	83.8
0.95			109.2[c]	116.9		82.3
Overall Mean		236.2	122.8		76.2	83.9

[a]Values not taken into consideration either for group mean or overall mean.

[b]Calculated from isoconversion plots for heating rates 4°, 6° and 10°/min.

[c]Calcutated from isoconversion plots for heating rates 2°, 4° and 6°/min.

[d]Calcutated from isoconversion plots for heating rates 4° and 6°/min.

[e]Calcutated from isoconversion plots for heating rates 2°, 4° and 6°/min.

nism tends to change with progress of dehydration. To examine this aspect the E values have been divided into two groups, namely α = 0.1–0.35 and α = 0.5–0.9 leaving the value at α = 0.4 as the possible transition point. This division, though appears arbitrary, is based on the reasonable range of E values for any given mechanism. The mean E values for these two groups are 317 and 143 kJ/mol, respectively, which are used to calculate θ values for the three heating rates according to eq. (9). The mean θ values at different fractional conversions (α) are shown in Table 3. Finally, the mean θ values are used to calculate the real or isothermal time required to reach different levels of α at three temperatures (370, 375 and 380 K) within the reaction step according to eq. (14). The most probable mechanistic model (Table 4) that may be operative in the dehydration process is then determined from the best linear fit of $g(\alpha)$ vs time and the results are shown in Table 5. A suitable computer program written in LOTUS

Table 3. Average values of reduced time θ calculated from different heating rates using the corresponding mean E values in Table 2

	Dehydration in static air				Dehydration in flowing N_2 atmosphere	
	2nd step (θ values calcd. are based on)		3rd step (θ values calcd. are based on)		2nd step (θ values calcd. are based on overall mean E value (min × 10^{10})	3rd step (θ values calcd are based on overall mean E value (min × 100)
(α)	Two separate mean E values (min × 10^{45})	Overall mean mean E values (min × 10^{32})	Two separate mean E values (min × 10^{14})	Overall mean E values (min × 10^{14})		
0.10	1.614	0.093	0.127	0.392	0.597	
0.20	4.553	0.179	0.179	0.546	0.801	
0.25	6.019					
0.30	10.565	0.348	0.233	0.708	1.019	2.384
0.35	15.873					
0.40		0.619	0.302	0.908	1.277	2.856
0.50	0.113	0.966	0.376	1.122	1.624	3.302
0.60	0.147	1.561	0.463	1.373	1.918	3.844
0.70	0.186	2.337	7.785	1.536	2.318	4.524
0.80	0.233	3.507	9.251	1.841	2.922	5.476
0.90	0.278	5.466	10.830	2.173	3.878	6.893
0.95			12.440	2.512		8.026

Table 4. Some important mechanistic equations (models) used in the study of the kinetics of solid-state reactions

Model code	Name of model equations	Equations in their integrated form, $g(\alpha)$
	Diffusion-controlled models	
*D*1	(i) One dimensional	α^2
*D*2	(ii) Two dimensional	$(1-\alpha)\ln(1-\alpha)+\alpha$
*D*3	(iii) Three dimensional (Jander's equation)	$[1-(1-\alpha)^{1/3}]^2$
*D*4	(iv) Three dimensional (Ginshtling and Braunshtein equation)	$1-2/3\alpha-(1-\alpha)^{2/3}$
	Nucleation growth controlled models	
Am	(i) Avrami-Erofee'v equation With m = 1.5, 2, 3, and 4	$[-\ln(1-\alpha)]^{1/m}$
*F*1	(ii) First order reaction (Random nucleation)	$-\ln(1-\alpha)$
Rn	Contracting phase boundary (i) Spherical geometry (n = 3) (ii) Cylindrical geometry (n = 2)	$1-(1-\alpha)^{1/n}$

1-2-3 has been used to extract the regression parameters for different models.

It is sometimes observed that more than one model give almost similar highest correlation coefficient (R^2). In such case it is necessary to look for minimum standard deviation or even for minimum intercept value for discrimination of the best fit model. Taking all these into consideration it can be seen from Table 5 that in the initial stage (α = 0.1–0.35) Zuravlev, Lesokhin and Tempelman (ZLT) model fits best. The model is based on the assumptions that (i) the diffusion takes place through the growing product layer and (ii) the reaction rate is proportional to the activity of the unreacted solid. In othe words, it is a combination of diffusion and progress of the reaction interface controlled model, both in respect of spherical geometry. As the reaction proceeds the mechanism changes to contracting phase boundary, also with spherical geometry (*R*3) i.e. from periphery to the center at the later stage of dehydration (α = 0.5–0.9). However, when the second step is considered as a whole, diffusion appears to be slower than interface advance and *D*4 is found to be the best-fit model, but with slightly lower correlation coefficient. This generally occurs when the coating of the product phase formed in the initial stage has fewer cracks, fissures etc. to allow free escape of H_2O molecules.

Fig. 5 illustrates the plot of α vs T for the third step of dehydration in static air at different heating rates and Fig. 6 represents the corresponding isoconversion plots. It may be noted from Fig. 6 that for α = 0.1–0.6 the linear behavior is followed at heating rates 4°, 6°, 10°/min whereas for α = 0.7 – 0.95 the linear behavior is followed at 2°, 4° and 6°/min. The E values obtained from the above two

Table 5. Kinetic models and Arrhenius parameters derived from the linear relationship between either reduced time θ or real time t and α at different temperatures and for different steps of dehydration of $MnCl_2.4H_2O$ in air as well as in N_2 environment

Steps of dehydration	Range of av. θ values (min)	α range	Temperature ture range (K)	Kinetic model (code)	R^2 on g(α) vs t	Arrhenius parameters		
						E kJ/mol	log A min	R^2
Dehydration in static air :								
2nd step	1.614–15.873 $\times 10^{-45}$	0.1–0.35	370–380	ZLT	0.9992	317.7	42.24	1.0
do	1.125–2.984 $\times 10^{-19}$	0.5–0.9	370–390	$R3$	0.9996	142.9	18.27	1.0
do	0.928–5.466 $\times 10^{-32}$	0.1–0.9	370–390	$D4$	0.9974	234.4	30.29	1.0
3rd step	0.127–0.463 $\times 10^{-14}$	0.1–0.6	435–445	$F1$	0.9995	126.6	14.36	1.0
do	7.785–12.44 $\times 10^{-14}$	0.7–0.95	440–450	$R3$	0.9972	117.0	12.83	1.0
do	0.392–2.512 $\times 10^{-14}$	0.1–0.95	435–450	$R2$	0.9982	121.4	13.37	1.0
Dehydration in flowing nitrogen environment :								
2nd step	0.597–3.878 $\times 10^{-10}$	0.1–0.9	370–390	$F1$	0.9980	76.1	9.81	1.0
3rd step	2.384–8.026 $\times 10^{-10}$	0.3–0.95	440–455	$A1.5$	0.9992	83.7	9.42	1.0

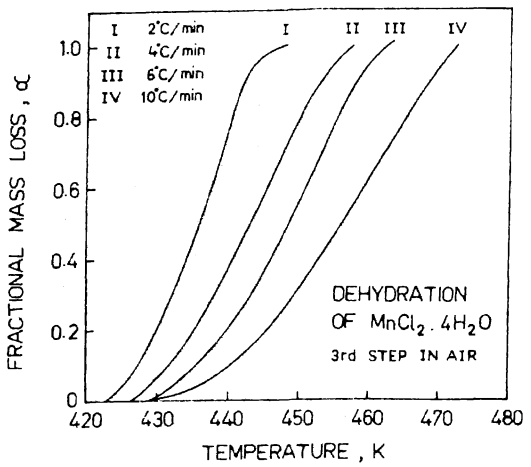

Fig. 5. Plot of α vs T for the third step of dehydration tetrahydrate in air at different heating rates.

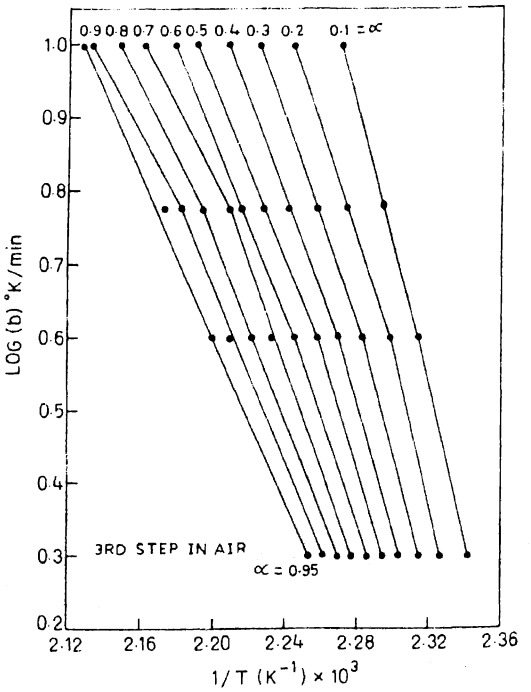

Fig. 6. Plot log (heating rate) vs $1/T$ at different leavels of α i.e. isoconversion plot for the thrid step of dehydration in air.

groups of linear plots comprising at least three heating rates do not show much variation with α as can be seen from Table 2. The corresponding mean E values are used to calculate θ values at different heating rates from which mean θ values are obtained for different values of α. An attempt has been made to test most probable mechanisitic model from the best linear fits of either $g(\alpha)$ vs θ or $g(\alpha)$ vs isothermal time t at three different temperatures within this step. The results are shown in Table 5.

In the third step of dehydration in air the rate of diffusion of H_2O vapour increases as the product obtained after the second step of dehydration is considerably dried-up and tends to develop more cracks, fissures etc. so that a first order growth controlled model ($F1$) tends to be the rate-controlling mechanism in the initial stage (α = 0.1–0.6). Like the second step of dehydration the mechanism changes to $R3$ at the later stage (α = 0.7–0.95). However, when the entire step is considered as a whole (α = 0.1–0.95) with a mean E value of 122.8 kJ/mol, progress of the product/reactant interface still appears to be the primary mechanism, but with different geometry ($R2$ model).

Like the static air environment the first step of dehydration in flowing nitrogen atmosphere also does not follow the linear isoconversion plot of log b vs $1/T$ for the entire conversion range. Therefore, no attempt has been made to study the kinetics of this step. Fig. 7 shows the plot of α vs T at different heating rates for the second

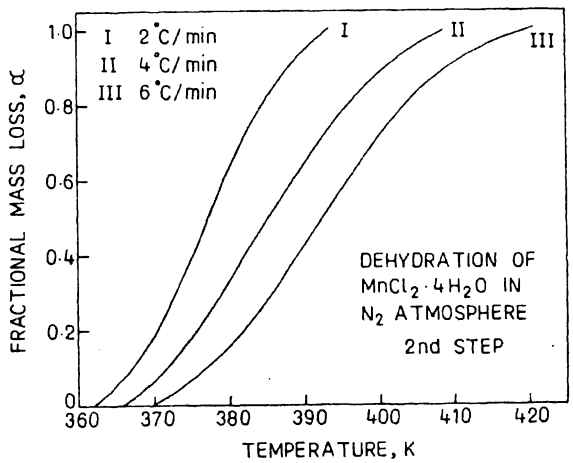

Fig. 7. Variation of α with temperature (T) at different heating rates for the second step of dehydration of tetrahydrate salt in nitrogen atmosphere.

step dehydration in flowing N_2 atmosphere. The data derived from this figure are used to construct the corresponding plot of log (b) vs $1/T$ for different values of α as illustrated in Fig. 8. The figure shows that in the initial stage (α = 0.1–0.4) the linear behavior is not followed for the three consecutive heating rates, but follows in the later stage of conversion (α = 0.5–0.95). However, closely similar slope values of the linear plots at the heating rates of 4° and 6°/min in the initial stage with those in the later stage for all the heating rates suggest possible similar mechanism at higher heating rates. Therefore, taking into consideration the E values obtained from the slopes of

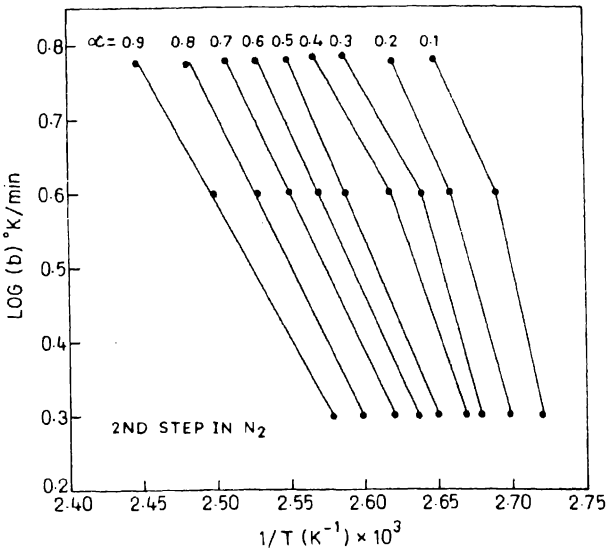

Fig. 8. Plot of log (heatig rate) vs $1/T$ at different levels of α for the second step of dehydration in nitrogen atmosphere.

the linear plots between 4° and 6°/min at α = 0.1–0.4 along with those obtained from the later stage (α = 0.5–0.95) comprising all the three heating rates a single average E value (76.2 kJ/mol) can be obtained for the entire second step of dehydration in N_2 environment. Proceeding in the same way as described above in the case of dehydration in air mean reduced time θ and real or isothermal time t are calculated for different values of α. An appropriate mechanistic model is then looked for from the best fit of $g(\alpha)$ vs θ or t. It is observed that first order growth process of randomly nucleated product phase ($F1$) fits the data best for the second step of dehydration in flowing N_2 atmosphere.

Figs. 9 and 10 show α vs T at different heating rates and the corresponding isoconversion plots, respectively, for the third stage of dehydration of $MnCl_2.4H_2O$ in flowing N_2 environment. Unlike the second step linear relationship is observed in the isoconversion curves for the entire α range from 0.1 to 0.95 comprising the three heating rates (4°, 6° and 8°/min). The decreasing E values as given in Table 2 suggest change in mechanism during the course of dehydration. However, neglecting the two high E values at α = 0.1 and 0.2, the average E value is 84.0 kJ/mol. The corresponding mean θ values are given in Table 3. Following the same procedure as described above, it is observed that nucleation and growth model fits the data best, but with little higher order ($A1.5$) than for step 2.

Most of the solid state dehydration reactions follow either Avrami-Erofeev equation of nucleation and growth

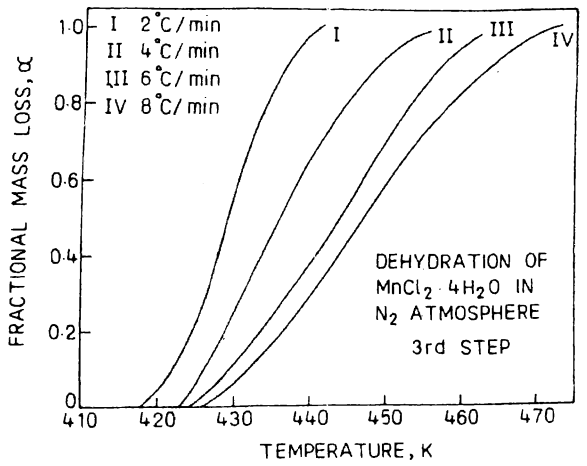

Fig. 9. Variation of α with temperature (T) at different heating rates for the third step of dehydrtion of tetrahydrate salt in nitrogen atmosphere.

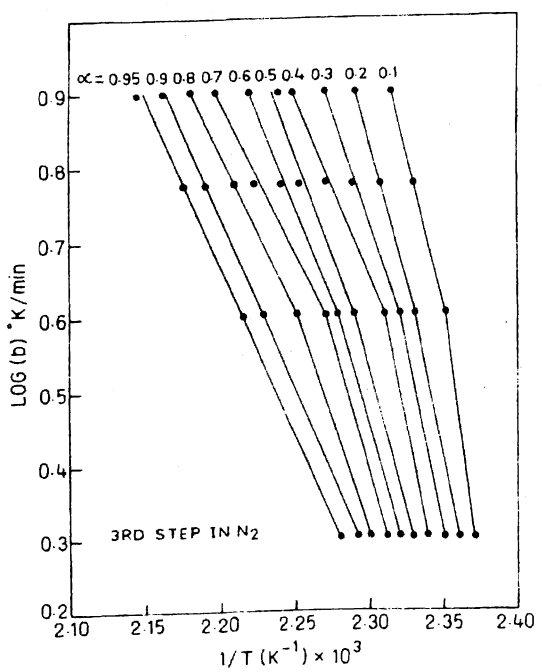

Fig. 10. Plot of log (heating rate) vs $1/T$ at different levels of α for the third step of dehydration in nitrogen atmosphere.

(*Am*) or advancing reaction interface (*Rn*) as kinetic model (Table 4). Such kinetic obediences can be interpreted in relation to reaction morphology i.e. the reaction proceeds with the progress of boundary between reactant/product which in turn depends upon the nucleation and growth of the product phase. Consequently, the correlation coefficient for any model belonging to one group is sometimes very close a model in the other group. This makes the selection of appropriate model sometimes a difficult task.

Experimental

Materials : Freshly procured reagent grade $MnCl_2 \cdot 4H_2O$ (E. Merck) was ground in an agate mortar and transferred to an 20 ml sample bottle and stored in a desiccator for subsequent use. Chemical analysis shows that the original sample contains 4.2 moles of water per mole of $MnCl_2$, but on storage in the desiccator the water mole decreased to 3.8. However, when the sample is exposed to atmosphere during weighing, loading in the instrument etc. some moisture may possibly be absorbed.

Method : Simultaneous DTA/TG of the sample was carried out in a Shimadzu (Japan) DT-40 Thermal Analyzer using 15–20 mg sample mass. The heating rate was varied between 2°/min to 10°/min. All the experiments were carried out in alumina microcrucibles under static air (self-generated atmosphere) as well as under flowing nitrogen (50 ml/min) environments.

The instrument was calibrated by carrying out thermolysis of a number of pure standard substances whose heats of thermal transformation/decomposition are known[14]. For this purpose heating rate was kept fixed at 10°/min and sample weight at 15 mg. The area within DTA peak was estimated by the square counting method using tracing graph paper. The calibration procedure is followed only under static air environment.

Acknowledgement

The author is thankful to his former colleague Dr. S. K. Mishra, Pool Scientist, R.R.L., Bhubaneswar, for his help in computer programming.

References

1. M. E. Brown, D. Dollimore and A. K. Galwey in "Comprehensive Chemical Kinetics", eds. C. H. Bamford and C. H. F. Tipper, Elsevier, Amsterdam, 1980, Vol. 22, Chap. 4, pp. 115-125.
2. A. K. Galwey, *J. Thermal Anal.*, 1992, **38**, 99.
3. A. K. Galwey, *J. Thermal Anal.*, 1994, **41**, 267.
4. E. I. Simmons and W. W. Wendlandt, *Thermochim. Acta*, 1971, **3**, 25.
5. J. Ribas, A. Escuer, M. Serra and R. Vicente, *Thermochim. Acta*, 1986, **102**, 125.
6. M. A. Mohamed and S. A. Halawy, *J. Thermal Anal.*, 1994, **41**, 147.
7. S. Stopic, I. Ilic and D. Uskokovic, *J. Sci. Sintering*, 1994, **26**, 145.
8. H. Tanaka and N. Koga, *J. Thermal Anal.*, 1988, **34**, 685.
9. S. K. Mishra and S. B. Kanungo, *J. Thermal Anal.*, 1992, **38**,

2417.

10. S. B. Kanungo and S. K. Mishra, *Thermochim. Acta*, 1994, **241**, 171.
11. S. K. Mishra and S. B. Kanungo, *J. Thermal Anal.*, 1992, **38**, 2437.
12. S. B. Kanungo and S. K. Mishra, *J. Thermal Anal.*, 1996, **46**, 1487.
13. S. B. Kanungo and S. K. Mishra, *J. Thermal Anal.*, 1997, **48**, 385.
14. W. W. Wendlandt, "Thermal Analysis", 3rd. ed., John Wiley & Sons, 1986, pp. 276-278.
15. J. Sestak, "Thermophysical Properties of Solids", 'Comprehensive Analytical Chemistry', Vol. XII, Part D, Elsevier, New York, 1984.
16. J. Sestak (Ed.), "Reaction Kinetics by Thermal Analysis", Special issue of *Thermochim. Acta*, Elsevier, Amsterdam, 1992, **203**, pp. 1-529.
17. T. Ozawa, *Bull. Chem. Soc. Jpn.*, 1965, **38**, 1881.
18. J. H. Flynn and L. A. Wall, *J. Polymer Sci., Part A*, 1966, **4**, 323.
19. C. D. Doyle, *J. Appl. Polym. Sci.*, 1962, **6**, 639.
20. T. Ozawa, *Thermochim. Acta*, 1992, **203**, 159.